Proceedings of the ASME 2017 Dynamic Systems and Control Conference
DSCC2017
October 11-13, 2017, Tysons, Virginia, USA

DSCC2017-5254

INVESTIGATION OF NANOSCALE POROELASTICITY OF EUKARYOTIC CELLS USING ATOMIC FORCE MICROSCOPY

Keyvan Mollaeian

Dept. of Mechanical Engineering
Iowa State University
Ames, Iowa, 50011, USA

Yi Liu

Dept. of Mechanical Engineering
Iowa State University
Ames, Iowa, 50011, USA

Juan Ren*

Dept. of Mechanical Engineering
Iowa State University
Ames, Iowa, 50011, USA
Email: juanren@iastate.edu

Abstract

Intracellular network deformation of the cell plays an important role in cellular shape formation. Recent studies suggest that cell reshaping and deformation due to external forces involves cellular volume, pore size, elasticity, and intracellular filaments polymerization rate changes. This behavior of live cells can be described by poroelastic models because of the porous structure of the cytoplasm. In this study, the poroelasticity of human mammary basel/claudin low carcinoma cell (MDA-MB-231) was investigated using indentation-based atomic force microscopy. The effects of cell deformation (i.e., indentation) rate on the poroelasticity of MDA-MB-231 cells were studied. Specifically, the cell poroelastic behavior (i.e., the diffusion coefficient) was quantified at different indenting velocities (0.2, 2, 10, 20, 100, 200 μm/s) by fitting the force-relaxation curves using a poroelastic model. It was found that the in general the MDA-MB-231 cells behaved poroelastic, and they were less poroelastic (i.e., with lower diffusion coefficient) at higher indenting velocities due to the local stiffening up caused by faster force loads. Poor poroelastic relaxation was observed when the indenting velocity was lower than 10 μm/s due to the intracelluar fluid redistribution during the slow indenting process to equilibrate the intracellular pressure. Moreover, the measurement results showed that the pore size reduction caused by local stiffening at faster indenting velocities is more dominant than the Young's modulus in affecting the cell poroelasticity.

*Address all correspondence to this author.

Introduction

Nowadays, attention toward cell rheology is growing due to the sensitivity of cell shape and deformation to external and internal biomechanical stimulation. For example, internal induced-forces due to biochemical interaction, intracellular organelle transport [1], transcriptional change of genes [2], and signaling pathways [3] proceed to elongation of the cells and cell cycling. Moreover, integrin-mediated focal adhesion [4, 5], ion channels [6], and cytoskeleton of the cell [7, 8, 9] are responsive to extracellular forces applied on the cell. As cytoplasm forms the largest part of a cell by volume, its biomechanical property plays a key role in cell rheology by dictating the cell deformation magnitude and cell shape change rate. Therefore, investigating the biomechanical behavior of the cytoplasm is crucial in achieving in-depth understanding of cell rheology. Furthermore, as it is widely found that living cells probe, react, and adapt to external mechanical stimulation [10, 11], studying the mechanical properties of cytoplasm also promotes the modeling and quantification of the transduction of external mechanical stimulation into intracellular mechanical changes.

Classical mechanical models have been implemented to biomechanics investigation of cell cytoplasm. To study the mechanics of live cell structure (e.g., cell membrane and cytoskeleton), solid mechanics models, such as the Hertizan model and the Sneddon model were used to describe the contact mechanics between an elastic indenter and living cells by assuming the latter as an elastic isotropic body, and the contact is purely repulsive [12, 13]. Due to the existence of attractive forces (e.g,

van der Waals forces) when the indenter is brought into close proximity with the cells, the Johnson-Kendall-Roberts (JKR) and the Derjaguin-Muller-Toporov (DMT) models were then used to incorporate the effect of adhesion in Hertzian contact by taking the thermodynamic work of adhesion into account [14, 15, 16]. The power-law structural damping model [17, 18] was used for studying the viscoelasticity and the dynamic behavior of adherent cells [19]. However, these models are not adequate enough to describe the biomechanical behavior of both the liquid flow (e.g., the cytosol) and the viscoelastic network (e.g., the cytoskeleton) —the biophasic nature of the cytoplasm. Therefore, a poroelastic model was implemented to study the biomechanics of cytoplasm, in which the cytoplasm was considered as a biphasic material consisting of a porous elastic solid meshwork (cytoskeleton, organelles, macromolicules) bathed in an interstitial fluid (cytosol) [20, 21, 10]. In the poroelastic model, the response of cells to external force load depends only on the poroelastic diffusion coefficient, D, which is determined by E the drained elastic modulus, ξ the pore size of the cytoskeleton meshwork, and μ the viscosity of the cytosol [10, 22, 23].

Poroelasticity studies of eukaryotic cells have been performed by atomic force microscopes (AFMs) because of AFM's unique capability of applying force stimuli and then, measuring the sample response at specific locations in a physiologically friendly environment with piconewton force and nanometer spatial resolutions [24, 25]. Wu et al. (1998) found that L929 cell structure was recovered during the relaxation of the AFM tip on the cell [26]. Hu el al. (2010) reported that interaction force between the AFM tip and the hydrogels was decreased during relaxation of the tip on the sample which led to deformation of the hydrogels [27]. Tavakoli Nia et al. (2011) noted the poroelastic behavior of cartilage during relaxation experiment using AFM [28]. It has been noted that the mechanical response of fluid-filled materials, like cells, depends on the time and length scales of the measurements and the mechanical deformation of the materials changes during the entire experimental time span [29]. Moeendarbary et al. (2013) investigated the poroelastic behavior of the cell using micro bead when the approach velocity was 10 μm/s, and it was found that the components of the cells including actin, microtubules, myosin, and intermediate filaments affect the diffusion coefficient of the cell [10]. However, since the cytoplasm of a live cell is highly heterogeneous and consists of a multi-layer structured viscoelastic cytoskeleton (i.e., velocity dependent), the cytoplasm poroelasticity quantified in previous work was limited to the specific measurement specifications and physical conditions (e.g., indenter size, approach velocity, and indentation depth). Particularly, due to the biphasic nature of live cells, the cell deformation rate (i.e., the AFM probe approach velocity) affects the measured cell stiffness significantly [10,30], and the deformation/indentation depth range determined the layers of the cells triggered and measured during the mechanical quantification [31, 32]. Thus, to achieve in-depth understanding of the cell rheological behavior, study of the poroelastic behavior of cytoplasm under different external excitation conditions is necessary.

In this study, we investigated the contribution of external force conditions to cellular rheology of human mamary basel/claudin low carcinoma cell at nanometer scale using AFM. Specifically, the cells were excited under forces with different indenting velocities, and the poroelasticity diffusion coefficient was then quantified for each velocity by fitting the force-relaxation curve using an empirical poroelastic model. Furthermore, to study the effect of internal cell structural property on the cell poroelastic relaxation, we examined the correlation between the poroelasticity diffusion coefficient and the Young's modulus of the cells for each measured condition.

Materials and Methods

Chemicals

The human mamary basel/claudin low carcinoma cell line (MDA-MB-231) was purchased from American Type Culture Collection (ATCC, Rockville, MD, USA). Dubecco's Modified Eagles Medium (DMEM) was purchased from Sigma Aldrich (St. Louis, MO, USA). Fetal bovine serum and penicillin-streptomycin were obtained from Gibco (Grand Island, New York, USA).

Cell culture and treatment

MDA-MB-231 cells were grown in DMEM containing 10 % fetal bovine serum (FBS) and 1 % penicillin-steptomycin (pen-strep). For the AFM measurement, the cells were seeded at a density of 2.0×10^4 cells/ml on 35 mm dishes (Falcon, Durham, NC, USA) and cultured for 24 hours at 37 °C in 5 % CO_2 incubator. Before the measurement, the existing medium in the dishes was replaced by fresh one to remove dead and loosely attached cells.

Atomic Force Microscopy (AFM) measurement

AFM measurement was performed at room temperature in aforementioned fresh cell culture medium using a Bruker BioScope Resolve AFM (Santa Barbara, CA, USA), which was integrated with an inverted optical microscope (Olympus, IX73, Japan). MLCT-BIO-DC-C (Bruker, Camarillo, CA) probe was used to measure the cells, and the spring constant of 0.03 N/m was acquired using thermal tune approach [33]. During the experiment, the AFM probe (guided by the optical microscope camera) was in contact with the cells at locations away from the top of the cells to avoid the nucleus effect. All of the

AFM drive voltage and sensor data were acquired using an NI PCIe-6353 DAQ board (National Instrument, Austin, TX, USA) with Matlab Simulink Desktop Real-Time system (Mathworks, MA, USA).

To investigate the effect of indentation speed (i.e., AFM probe approaching velocity) on poroelasticity of MDA-MB-231 cells, the AFM probe was brought into contact with the cells at six different speeds (0.2, 2.0, 10.0, 20.0, 100.0, and 200.0 μm/s) until reaching a target indentation at 960 nm (Fig. 1 (I-II)), and then the AFM z-piezo displacement was maintained constant at the corresponding value for 1 sec to acquire the force relaxation data (Fig. 1 (II-III)). A proportional-integral (PI) feedback control loop was implemented to control the AFM piezo displacement. For each desired indentation velocity and indentation depth, the force measurement was performed on six different cells using the same AFM probe.

Nanomechanical quantification of MDA-MB-231 cell

Indentation depth was calculated by subtracting the cantilever deflection, $d(t)$, from the AFM z-piezo displacement [34], $z(t)$ i.e.,

$$\delta(t) = z(t) - d(t). \tag{1}$$

Since the AFM probe used had a conical shape, the Young's Modulus of MDA-MB-231 cells was quantified using the Sneddon model [35], i.e.,

$$F(t) = \frac{2}{\pi}\tan(\alpha)\frac{E}{1-\nu^2}\delta(t)^2. \tag{2}$$

where α and ν are the tip opening angle and the Poisson ratio of the cell, respectively. Additionally, $\nu = 0.3$ [10, 36] was used for elasticity measurements.

Cellular poroelasticity measurement

As the cell size (>30 μm) was more than three orders of magnitude larger than the AFM tip radius (25 nm), the probe-cell interaction could be approximated as a poroelastic half-space indented by a conical indenter, and the following empirical poroelastic model obtained by finite-element-analysis was used for analyzing the cell poroelasticity [27]:

$$\frac{F(t)-F_f}{F_i-F_f} = 0.493e^{-0.822\sqrt{\frac{Dt}{a^2}}} + 0.507e^{-1.348\frac{Dt}{a^2}}. \tag{3}$$

where F_i and F_f are initial and final forces in the relaxation portion of the force-time curve, respectively. D is the diffusion coefficient. The probe-cell contact size, a, can be quantified using the indentation depth as:

$$a = \frac{2}{\pi}\bar{\delta}\tan(\alpha). \tag{4}$$

where $\bar{\delta}$ is the indentation depth at the beginning of the force-relaxation process (i.e., the indentation caused by the displacement of the AFM piezo), and α is the half opening angle of the conical shaped AFM probe.

Curve fitting and statistical analysis

Relaxation portions of collected force-time curves from AFM were fitted by the poroelastic model (Eq. 3) using Matlab. Each experiment was performed on 6 different cells to validate the results. Each force-relaxation curve was fitted and the RMS fitting error was included in the results to demonstrate the measurement consistency.

Results and discussion

Porelastic behavior of living cells

First, the experiment results demonstrated that living cells exhibited poroelastic behavior. As shown in Fig. 2, the probe-cell interaction force started to decrease once the probe was rested on the cell surface following the indenting process, and went through a rapid exponential decay during the 1 sec relaxation measurement. This observation is consistent with the previous studies on other cell types [10, 26]. Indeed, the poroelasticity model (Eq. 3) fitted the force-relaxation curve well with the relative RMS fitting error ranging between 2.5–10.4 %. These indicate that the force decrease during the relaxation corresponds to cellular poroelastic behavior. As can be seen in Figs. 2 and 3 during the 1 sec relaxation, the force reduced by 08–63 % for all the measurements but the indentation increase was less than 6 %, indicating that the force-relaxation data were collected under approximately constant applied intracellular strain. Therefore, the force relaxation (i.e., the force decrease) was primarily caused by intracellular fluid (e.g., cytosol) redistribution within the cytoplasm. Although the probe was rested following the indenting process, the applied compression on the cell caused the intracellular liquid to move out of the probe-cell contact region through the porous structured cytoskeleton to equilibrate, and consequently, a reduction of the probe-cell interaction force.

To further study how the measurement conditions affect cell poroelastisity, we measured the force–relaxation curve under different indenting velocities.

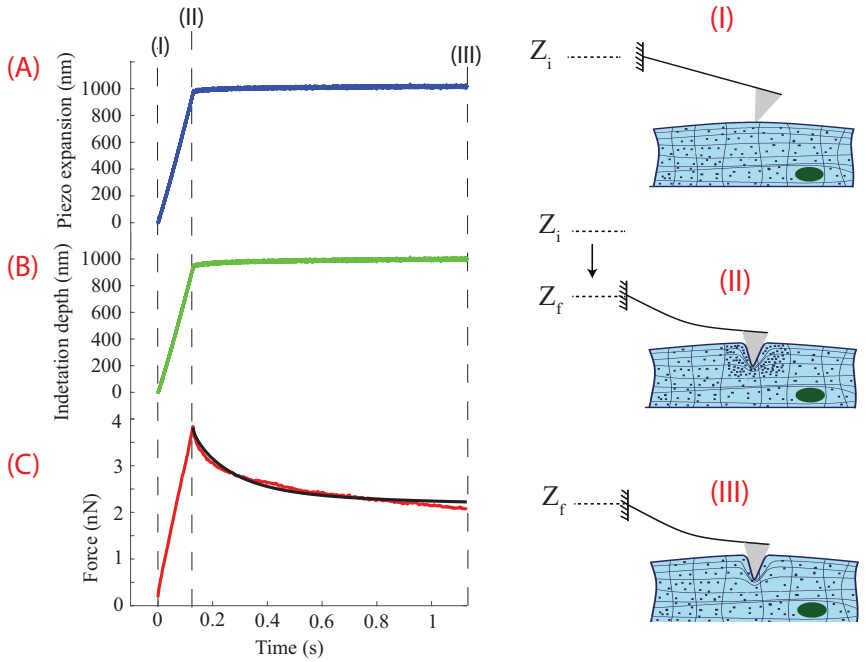

FIGURE 1. A,B,C) The AFM piezo displacement, the indentation depth, and the probe-sample interaction force during the poroelasticity measurement are demonstrated. I) At the beginning of the measurement the AFM tip was in contact with the surface of the cell with zero velocity. II) Indenting: the AFM probe indented the cell at a constant velocity until the desired indentation was reached. Multiple layers and the intracellular fluid of the cell were compressed during this loading process. III) Relaxation: the AFM probe rested on the cell, and the intracellular fluid redistributed to equilibrate the cell internal pressure, while the AFM z-piezo displacement was maintained at a constant since the end of the indenting process. The force-relaxation curve (the black solid curve in (C)) was then fitted using the poroelastic model

Effect of indenting velocity on poroelasticity of the cell

Six different indenting velocities (0.2, 2.0, 10.0, 20.0, 100.0, and 200.0 μm/s) were tested with the same targeted AFM indentation depth of 960 nm, and the force relaxation measurement was performed on six different cells for each velocity. The measured force relaxation curves were then fitted using Eq. 3, yielded a relative RMS fitting error in the range of 2.5 %–14 % for all of the 36 measurements. The results indicated that the cell poroelastic relaxation is more significant at higher approach velocities. Specifically, as shown in Figs. 2 and 3, the indentation increase and the force reduction were over 4 % and 40 %, with respect to their initial values (i.e., the indentation and force at the beginning of the relaxation), respectively, when the indenting velocity was higher than 10 μm/s. However, the indentation remained almost unchanged (with about 1 % increase), and the force only decreased at most 23 % for indenting velocities at 0.2 and 2 μm/s, indicating the probe-cell interaction was closer to equilibrium during the 1 sec relaxation process. In another word, the poroelastic relaxation phenomenon was more pronounced when the indenting velocity was higher than 10 μm/s. This is also confirmed by the normalized force-relaxation curve. The fitted force relaxation curves for different indenting velocities were normalized as $(F(t)-F_f)/(F_i-F_f)$ as shown in Fig. 4. The normalized force relaxation curves for the indenting velocities of 0.2 and 2 μm/s were different from those for the higher velocities (Fig. 4).

This observation agrees with the empirical poroelastic model (Eq. 3). According to Eq. 3, the poroelastic relaxation becomes more significant if the indenting velocity v is faster than the fluid efflux [10, 37], i.e., $v > \bar{\delta}/t_p$, where t_p is the timescale of the intracellular fluid movement and $t_p \sim a^2/D$. As the quantified diffusion coefficient (by fitting the force-relaxation curve using Eq. 3) for the targeted $\bar{\delta} \sim 960$ nm is in the range of 0.2–1.5 μm^2/s (see Fig. 5), the indenting velocity for poroelastic relaxation observation needs to satisfy $v > 7$ μm/s. Fig. 4 indicates that the timescale a^2/D was very close for each approach velocity $v > 7$ μm/s, i.e., the timescale of the intracelullar fluid movement $t_p \sim a^2/D$ was almost the same for all $v > 7$ μm/s, confirming that the intracellular fluid efflux was negligible for these approach velocities during the indentation process and contributed to the observed force relaxation. Therefore, the force relaxation immediately following AFM indentation was indeed caused by intracellular fluid efflux, and became more significant once the indenting velocity is faster than the fluid efflux rate. Particularly, at the indenting velocities lower than 7 μm/s, the intracellular fluid flew out of the probe-cell contact region to equilibrate the pore pressure during the approaching process

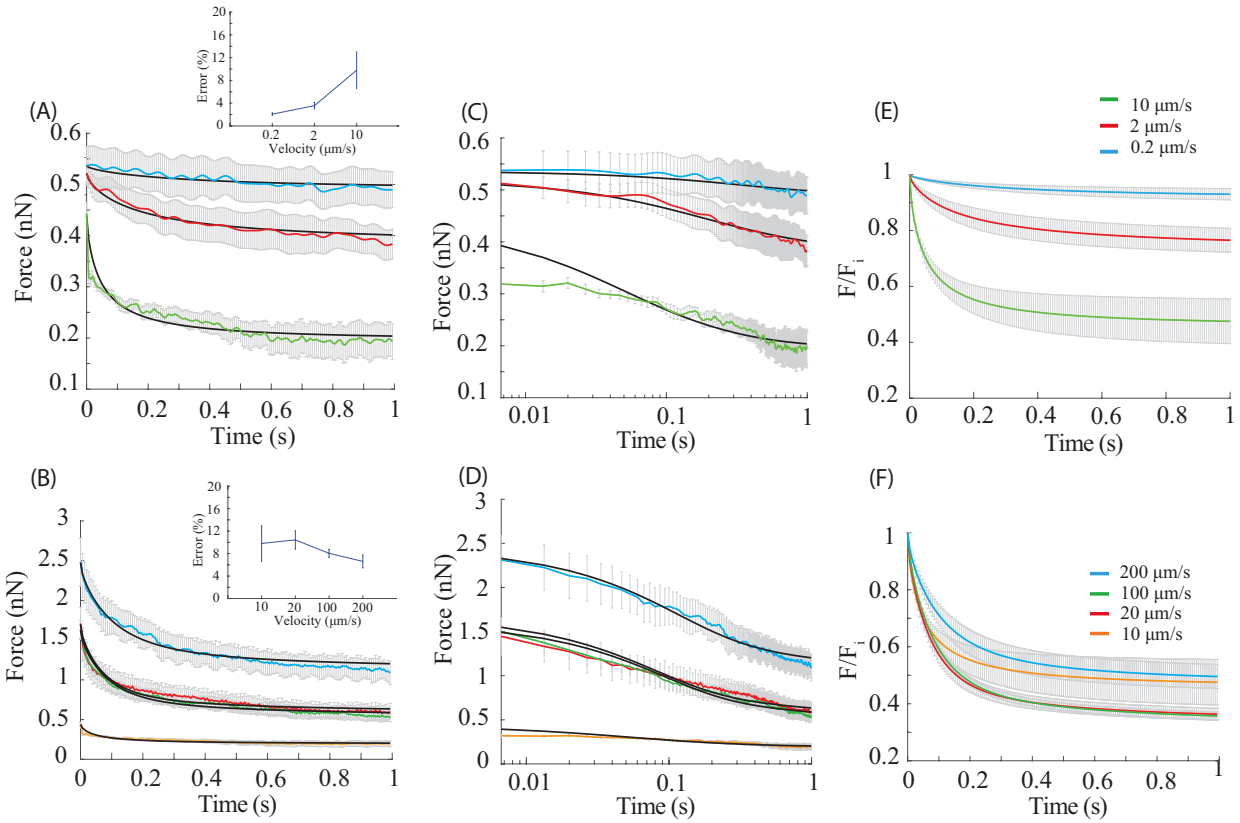

FIGURE 2. A) Force-relaxation curve for indenting velocities of 0.2, 2, and 10 μm/s when the targeted indentation depth was 960 nm. The mean value of the fitted curves for each velocity was shown as solid lines. The error bars denote the raw force data for each indenting velocity. B) Force-relaxation curves for indenting velocities of 10, 20, 100, and 200 μm/s when the targeted indentation was 960 nm. C, D) Log-Log plots of A) and B), respectively. E, F) Relative force reduction during the relaxation process of the poroelastic fitted results in A) and B), respectively.

and soon reached equilibrium (steady-state), which resulted in barely changed force and indentation, i.e., the cell behavior was more elastic other than poroelastic, during the relaxation measurement. On the contrary, the intracellular fluid was not able to respond fast enough during rapid indentation ($v > 7$ μm/s), and then efflux started to occur once the probe was rested on the cell to equilibrate the intracellular pressure, and led to a significant reduction of the probe-cell interaction force.

To further study the relation between the cytoskeleton elasticity (i.e., Young's modulus) and the poroelasticity, we fitted the force-indentation curve with the Sneddon contact model (Eq. 2) to quantify the Young's modulus E of the cells under different indenting velocities. The fitting results yielded a Young's modulus E ranging between 1.5–147 kPa monotonically increasing with the indenting velocity as shown in Figs. 5. This E vs. v trend is consistent with previous findings [30] as the cytoskeleton is highly viscoelastic and faster indenting velocities can increase the polymerization degree of the local actin, which further leads to local stiffening of the cytoskeleton [38, 10]. As a result, the increased actin polymerization and cytoskeleton stiffening may decrease the cytoskeleton pore size significantly, and further slows down the intracellular fluid efflux during the force relaxation process. This is confirmed in Fig. 2 (B) and (F), where the force reduction is smaller for higher indenting velocities during poroelastic relaxation for $v > 7$ μm/s (note that the cases for $v < 7$ μm/s are excluded since fluid efflux happened even before the relaxation started as discussed earlier). The trend of the quantified diffusion coefficient D is also consistent with the above discussion in Fig. 2, where D has an inverse relation with E for all $v > 7$ μm/s (see Figs. 5), as a higher value of D corresponds to more rapid fluid efflux. Note that this inverse relation between D and E doesn't conflict with the general recognized scaling law of diffusion coefficient: $D \sim E\eta^2/\mu$, where η is the pore radius of the cytoskeleton mesh work, and μ is the viscosity of the intracellular fluid (i.e., cytosol). Although a higher approach velocity resulted in an increase E, but the local cytoskeleton stiffening and actin polymerization caused the pore size to decrease, and led to an overall smaller D. This indicates that changes in

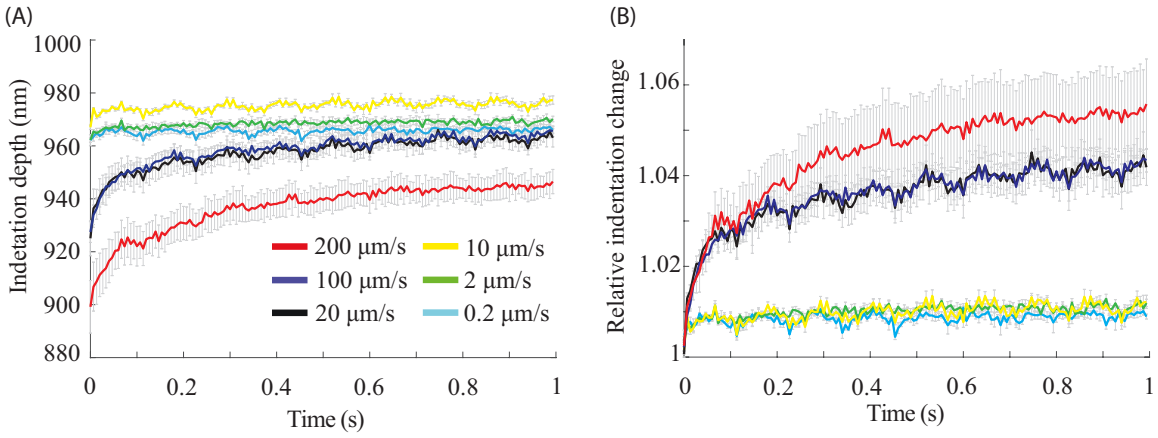

FIGURE 3. A) Indentation vs. time during the relaxation process: the indentation depth gradually increased when the probe was resting on the cell following the rapid indenting process B) Relative indentation change $\delta/\bar{\delta}$ during the relaxation process.

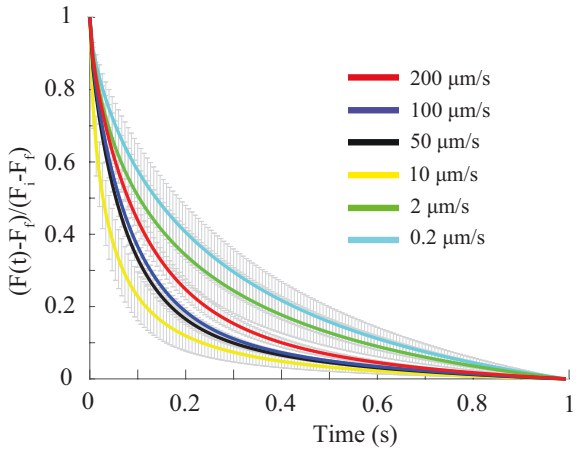

FIGURE 4. Normalized force reduction curve for different indenting velocities when the indentation depth was 960 nm. At the same time instant, lower normalized value denotes faster poroelastic relaxation.

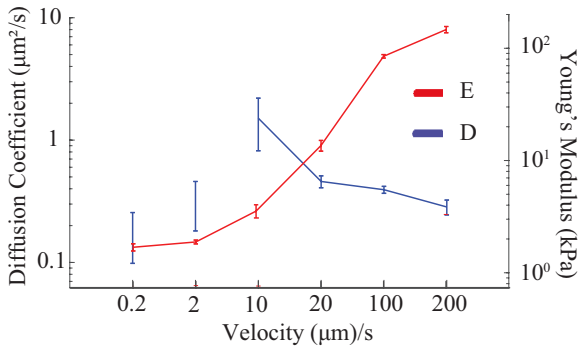

FIGURE 5. Poroelastic and elastic properties change in response to change in indenting velocity.

η were more dominant than the changes of E in affecting the cytoplasm poroelasticity, and thereby, the cell rheology. As it is known that live cells are highly heterogeneous, and the cell shows high nonlinearity in terms of mechanical responses to external force excitation [11, 39], future study will work on investigating the nonlinearity of cell poroelasticity.

Conclusion

In this study, the effects of indenting velocities on the poroelasticity of MDA-MB-231 cell cytoplasm were investigated. The poroelastic behavior of the cell was quantified for indenting velocities of 0.2, 2, 10, 20, 100, 200 μm/s by fitting force-relaxation curves with the poroelastic model. It was found that the cell had poor poroelastic behavior when the indenting velocity was lower than 10 μm/s due to intracellular fluid redistribution during the indenting process. Lower diffusion coefficient for faster indenting velocities confirmed poor poroelastic behavior of the cell due to local stiffening of the cell at faster velocities. Moreover, investigating the Young's modulus and the diffusion coefficient obtained under the above mentioned six indenting velocity suggested that the pore size reduction caused by local stiffening of the cell at faster velocities is more dominant that the cell Young's modulus in terms of affecting the cell poroelasticity.

Acknowledgment

The authors acknowledge the financial support from the National Science Foundation (NSF) CMMI-1634592. The authors also thank Dr. Ian Schneider for providing MDA-MB-231 cells.

REFERENCES

[1] Niclas, J., Allan, V. J., and Vale, R. D., 1996. "Cell cycle regulation of dynein association with membranes modulates microtubule-based organelle transport". *Journal of Cell Biology,* **133**(3), pp. 585–594.

[2] Coller, H. A., Grandori, C., Tamayo, P., Colbert, T., Lander, E. S., Eisenman, R. N., and Golub, T. R., 2000. "Expression analysis with oligonucleotide microarrays reveals that myc regulates genes involved in growth, cell cycle, signaling, and adhesion". *Proceedings of the National Academy of Sciences,* **97**(7), pp. 3260–3265.

[3] Elledge, S. J., 1996. "Cell cycle checkpoints: preventing an identity crisis". *Science,* **274**(5293), p. 1664.

[4] Balaban, N. Q., Schwarz, U. S., Riveline, D., Goichberg, P., Tzur, G., Sabanay, I., Mahalu, D., Safran, S., Bershadsky, A., Addadi, L., et al., 2001. "Force and focal adhesion assembly: a close relationship studied using elastic micropatterned substrates". *Nature cell biology,* **3**(5), pp. 466–472.

[5] Plotnikov, S. V., Pasapera, A. M., Sabass, B., and Waterman, C. M., 2012. "Force fluctuations within focal adhesions mediate ecm-rigidity sensing to guide directed cell migration". *Cell,* **151**(7), pp. 1513–1527.

[6] Hayakawa, K., Tatsumi, H., and Sokabe, M., 2008. "Actin stress fibers transmit and focus force to activate mechanosensitive channels". *J Cell Sci,* **121**(4), pp. 496–503.

[7] Mitrossilis, D., Fouchard, J., Guiroy, A., Desprat, N., Rodriguez, N., Fabry, B., and Asnacios, A., 2009. "Single-cell response to stiffness exhibits muscle-like behavior". *Proceedings of the National Academy of Sciences,* **106**(43), pp. 18243–18248.

[8] Colombelli, J., Besser, A., Kress, H., Reynaud, E. G., Girard, P., Caussinus, E., Haselmann, U., Small, J. V., Schwarz, U. S., and Stelzer, E. H., 2009. "Mechanosensing in actin stress fibers revealed by a close correlation between force and protein localization". *Journal of cell science,* **122**(10), pp. 1665–1679.

[9] Hayakawa, K., Tatsumi, H., and Sokabe, M., 2011. "Actin filaments function as a tension sensor by tension-dependent binding of cofilin to the filament". *J Cell Biol,* **195**(5), pp. 721–727.

[10] Moeendarbary, E., Valon, L., Fritzsche, M., Harris, A. R., Moulding, D. A., Thrasher, A. J., Stride, E., Mahadevan, L., and Charras, G. T., 2013. "The cytoplasm of living cells behaves as a poroelastic material". *Nature materials,* **12**(3), pp. 253–261.

[11] Schillers, H., Wälte, M., Urbanova, K., and Oberleithner, H., 2010. "Real-time monitoring of cell elasticity reveals oscillating myosin activity". *Biophysical journal,* **99**(11), pp. 3639–3646.

[12] Liu, K.-K., 2006. "Deformation behaviour of soft particles: a review". *Journal of Physics D: Applied Physics,* **39**(11), p. R189.

[13] Butt, H.-J., Cappella, B., and Kappl, M., 2005. "Force measurements with the atomic force microscope: Technique, interpretation and applications". *Surface science reports,* **59**(1), pp. 1–152.

[14] Johnson, K., Kendall, K., and Roberts, A., 1971. "Surface energy and the contact of elastic solids". In Proceedings of the Royal Society of London A: Mathematical, Physical and Engineering Sciences, Vol. 324, The Royal Society, pp. 301–313.

[15] Derjaguin, B. V., Muller, V. M., and Toporov, Y. P., 1975. "Effect of contact deformations on the adhesion of particles". *Journal of Colloid and interface science,* **53**(2), pp. 314–326.

[16] Wu, S., 1982. *Polymer interface and adhesion*. M. Dekker.

[17] Hildebrandt, J., 1969. "Comparison of mathematical models for cat lung and viscoelastic balloon derived by laplace transform methods from pressurevolume data". *Bulletin of Mathematical Biology,* **31**(4), pp. 651–667.

[18] Fredberg, J. J., and Stamenovic, D., 1989. "On the imperfect elasticity of lung tissue". *Journal of applied physiology,* **67**(6), pp. 2408–2419.

[19] Ren, J., Yu, S., Gao, N., and Zou, Q., 2013. "Indentation quantification for in-liquid nanomechanical measurement of soft material using an atomic force microscope: Rate-dependent elastic modulus of live cells". *Physical Review E,* **88**(5), p. 052711.

[20] Oster, G., 1989. *Cell motility and tissue morphogenesis*. Academic Press, New York.

[21] Guilak, F., and Mow, V. C., 2000. "The mechanical environment of the chondrocyte: a biphasic finite element model of cell–matrix interactions in articular cartilage". *Journal of biomechanics,* **33**(12), pp. 1663–1673.

[22] Charras, G. T., Mitchison, T. J., and Mahadevan, L., 2009. "Animal cell hydraulics". *Journal of Cell Science,* **122**(18), pp. 3233–3241.

[23] Charras, G. T., Coughlin, M., Mitchison, T. J., and Mahadevan, L., 2008. "Life and times of a cellular bleb". *Biophysical journal,* **94**(5), pp. 1836–1853.

[24] Binnig, G., Quate, C. F., and Gerber, C., 1986. "Atomic force microscope". *Physical review letters,* **56**(9), p. 930.

[25] Butt, H., Cappella, B., and Kappl, M., 2005. "Force measurements with the atomic force microscope: Technique, interpretation and applications". *Surface Science Reports,* **59**, pp. 1–152.

[26] Wu, H., Kuhn, T., and Moy, V., 1998. "Mechanical properties of l929 cells measured by atomic force microscopy: effects of anticytoskeletal drugs and membrane crosslinking". *Scanning,* **20**(5), pp. 389–397.

[27] Hu, Y., Zhao, X., Vlassak, J. J., and Suo, Z., 2010. "Using indentation to characterize the poroelasticity of gels". *Applied Physics Letters,* **96**(12), p. 121904.

[28] Nia, H. T., Han, L., Li, Y., Ortiz, C., and Grodzinsky, A., 2011. "Poroelasticity of cartilage at the nanoscale". *Biophysical journal,* **101**(9), pp. 2304–2313.

[29] Kalcioglu, Z. I., Mahmoodian, R., Hu, Y., Suo, Z., and Van Vliet, K. J., 2012. "From macro-to microscale poroelastic characterization of polymeric hydrogels via indentation". *Soft Matter,* **8**(12), pp. 3393–3398.

[30] CHENG, A. H.-D., 2014. "Fundamentals of poroelasticity". *Analysis and Design Methods: Comprehensive Rock Engineering: Principles, Practice and Projects,* **113**.

[31] Kasas, S., Wang, X., Hirling, H., Marsault, R., Huni, B., Yersin, A., Regazzi, R., Grenningloh, G., Riederer, B., Forro, L., et al., 2005. "Superficial and deep changes of cellular mechanical properties following cytoskeleton disassembly". *Cytoskeleton,* **62**(2), pp. 124–132.

[32] Iyer, S., Gaikwad, R., Subba-Rao, V., Woodworth, C., and Sokolov, I., 2009. "Atomic force microscopy detects differences in the surface brush of normal and cancerous cells". *Nature nanotechnology,* **4**(6), pp. 389–393.

[33] Hutter, J. L., and Bechhoefer, J., 1993. "Calibration of atomic-force microscope tips". *Review of Scientific Instruments,* **64**(7), pp. 1868–1873.

[34] Ren, J., Huang, H., Liu, Y., Zheng, X., and Zou, Q., 2015. "An atomic force microscope study revealed two mechanisms in the effect of anticancer drugs on rate-dependent youngs modulus of human prostate cancer cells". *PloS one,* **10**(5), p. e0126107.

[35] Sneddon, I. N., 1965. "The relation between load and penetration in the axisymmetric boussinesq problem for a punch of arbitrary profile". *International journal of engineering science,* **3**(1), pp. 47–57.

[36] Charras, G., Lehenkari, P. P., and Horton, M., 2001. "Atomic force microscopy can be used to mechanically stimulate osteoblasts and evaluate cellular strain distributions". *Ultramicroscopy,* **86**(1), pp. 85–95.

[37] Ibata, K., Takimoto, S., Morisaku, T., Miyawaki, A., and Yasui, M., 2011. "Analysis of aquaporin-mediated diffusional water permeability by coherent anti-stokes raman scattering microscopy". *Biophysical journal,* **101**(9), pp. 2277–2283.

[38] Rotsch, C., and Radmacher, M., 2000. "Drug-induced changes of cytoskeletal structure and mechanics in fibroblasts: an atomic force microscopy study". *Biophysical journal,* **78**(1), pp. 520–535.

[39] Fernández, P., Pullarkat, P. A., and Ott, A., 2006. "A master relation defines the nonlinear viscoelasticity of single fibroblasts". *Biophysical journal,* **90**(10), pp. 3796–3805.